ELSEVIER

Polymer 40 (1999) 397–406

polymer

Study of the molecular structure of PET films obtained by an inverse stretching process
Part 2: crystalline reorganization during longitudinal drawing

M. Vigny[a], J.F. Tassin[a,*], G. Lorentz[b]

[a]*Université du Maine, Chimie et Physique des Matériaux Polymères, UMR-CNRS 6515, Avenue Olivier Messiaen, 72085 Le Mans Cedex 9, France*
[b]*Rhône Poulenc, Centre de Recherches d'Aubervilliers, 52, Rue de la Haie Coq, 93308 Aubervilliers Cedex, France*

Received 6 February 1998; accepted 24 February 1998

Abstract

The transverse stretching, under a constant drawing force, of a one-way drawn poly(ethylene terephtalate) film has been studied. This type of stretching leads to an equilibrium deformation under load which increases mainly with the applied stress and to a lesser degree with temperature. The crystalline phase of such samples has been characterized using wide-angle X-ray diffraction. The orientation of the chain axis and the normal to the phenylene ring have been analysed as well as the crystalline size, as a function of the draw ratio and the stretching temperature. The crystallinity is constant during stretching. The orientation distribution of the chain axes as well as the length of the crystals shows that the crystals which were preferentially oriented with their *c*-axes along the first stretching direction rotate rapidly towards the actual draw direction and grow up in length as the stretching proceeds. At the same time, the length of the crystals aligned along the other direction of the film plane decreases rapidly, indicating a break-down of some of these crystals. The orientation in the crystalline phase is uniquely controlled by the draw ratio. No relaxation with temperature is observed. This stretching method is compared with the constant speed drawing of one-way drawn films, where no rotation of large crystallites can be detected.

Keywords: Molecular orientation; PET films; Biaxial drawing

1. Introduction

Poly(ethylene terephtalate) (PET) is a widely used polymer which undergoes, under controlled conditions above the glass transition temperature, stress-induced crystallization. Interesting and somewhat adjustable mechanical properties are obtained thanks to the development of molecular orientation during processing. There is, therefore, extensive interest in understanding the molecular structure and the organization which appears during industrial processes who generate biaxial orientation such as the injection stretch blow molding [1–3] or the biaxial stretching of sheets [4–19].

The present work focuses on the molecular behavior during one stretching step of an unusual succession of drawing stages, used in the so-called "inverse" biaxial stretching process of PET films. The first stretching consists of a constant speed drawing of an amorphous film transversally to the machine direction. In the second stage, the monodrawn film is stretched between rolls, i.e. longitudinally at constant stress and constant width. The last step consists in an high temperature thermosetting treatment. This process differs from the more classical "balanced" process by the exchange of the two stretching steps. In the "balanced" process a longitudinal drawing under constant force of the amorphous film [20,21] is followed by a transversal constant speed stretching [15–17].

Biaxially deformed films have been studied by several groups. Samples were obtained either under simultaneous [5,6] or sequential [7–9,11–14] stretchings carried out at constant drawing speed. To our knowledge, the transverse stretching under constant force of one-way drawn films has not been reported.

This paper follows a previous study [22] dealing with the first stretching stage of the industrial "inverse" process, i.e. the stretching, at constant drawing speed, under uniaxial–planar conditions of an amorphous PET film. The molecular orientation and crystalline morphology of model samples have been described and compared to amorphous samples stretched under constant load conditions like in the "balanced" process [20,21].

* Corresponding author.

0032-3861/98/$ - see front matter
PII: S0032-3861(98)00199-2

The present paper deals with an investigation of the orientational behavior of the crystalline phase of monodrawn films transversally stretched under various conditions of temperature and applied loads. Several mechanisms involved in the second stage of the "inverse" process will be described and compared with the second step of the balanced process. Almost the same strategy has been used as in previous studies. Model samples have been prepared on a laboratory scale stretching device and further characterized using various techniques. Hereafter, results obtained mainly using X-ray diffraction will be considered.

1.1. Definition of axes and orientation

In this paper, we choose X_1, as the first drawing direction; X_2 as the second drawing direction and X_3 as the direction normal to the plane of the film. These conventions will be used whatever the type of sample under consideration either from the "inverse" or "balanced" process. The orientation of any molecular direction u, with respect to any macroscopic direction X_i, will be quantified by the average value of the second order Legendre polynomial:

$$P_2^{u/X_i} = \frac{1}{2}\langle 3\cos^2\theta_{u,X_i} - 1\rangle \quad (1)$$

where θ_{u,X_i} is the angle between the axes u and X_i, and the brackets denote an average over all the molecular units.

Since the original samples are one-way drawn films along the X_1 direction, our study will focus on reorientation mechanisms along the second stretching direction i.e. X_2.

2. Experimental

2.1. Density determination

The density d was calculated from the mean refractive index $\bar{n}$ using the Lorentz–Lorenz equation:

$$d_{(g/cm^3)} = 4.047\frac{\bar{n}^2 - 1}{\bar{n}^2 + 2} \quad (2)$$

The mean refractive index has been deduced from the measurements of the three principal refractive indices of the stretched material using an Abbe refractometer under polarized light. To simplify and in the lack of better approximation, the crystallinity was determined by assuming a non-interpenetrated two-phase model despite the existence of a "mesophase" which is generally acknowledged [18,23–25]. This third phase corresponds to a densification of the amorphous phase just before crystallization or near the crystal interface. Under these simplifying conditions, the crystallinity ratio χ can be written as:

$$\chi = \frac{d - d_a}{d_c - d_a} \quad (3)$$

where d_c referred to the density of the crystalline phase and d_a the amorphous density. There were established to be 1.455 and 1.335 g cm^{-3}, respectively [26].

2.2. X-ray diffraction

Wide-angle X-ray diffraction has been used to characterize the orientations of various crystallographic directions as well as the averaged dimensions of crystalline blocks along these directions. In the following, the unit cell is chosen as that determined by Daubeny et al. [25].

The orientation of two series of crystallographic planes, defined by their Miller indices, was investigated: ($\bar{1}05$) whose plane normal is close to the chain axes direction and (100) whose plane normal is close to the benzene ring normal. A Huber wide-angle X-ray diffractometer was used to tilt the sample and measure the orientation of these two important molecular directions [22]. The X-rays (Cu Kα radiation) were produced with an Inel generator operated at 39 kV and 30 mA. A sample of roughly 200 μm was obtained by stacking several pieces of stretched films. The procedure and relationships used to obtain the order parameters P_2 are those detailed by Faisant et al. [15]. We only recall hereafter the main steps of the experiments. To determine the orientation in all space, two rotations are required: ϕ_0 (the out-of-plane rotation) is defined to be the angle between the scattering vector and a direction in the plane of the film and ϕ_p (the in-plane rotation) may be varied by rotating the film around its normal. For the ($\bar{1}05$) reflection, a transmission setup was used. The angle ϕ_p was chosen and ϕ_0 was varied from $-30°$ to $30°$ in steps of $2°$. ϕ_p values were taken every $2°$ around the principal direction X_1 and X_2 and every $5°$ elsewhere (ϕ_p is taken equal to zero when the scattering vector is parallel to X_1). The resultant intensity matrix $I(\phi_p, \phi_0)$ was corrected for the amorphous background and for changes of absorption with ϕ_0 as described in Ref. [15].

To collect data for the (100) reflection, a reflection geometry was used. ϕ_0 was first chosen and ϕ_p varied from $-20°$ to $200°$ in steps of $5°$. Values of ϕ_0 were chosen every $2°$ from $-60°$ to $60°$ ($\phi_0 = 0°$ corresponding to the in-plane rotation). The experimental intensity matrix was also corrected. The corrected intensity matrices were used to calculate by numerical integration the P_2 values.

The size of the crystallites in the direction normal to (hkl) planes, denoted L_{hkl}, has been determined from the angular broadening of the diffraction peaks using the Scherrer equation [15,20,26]. Considering as well the dimensions of the unit cell as the intense diffraction peaks and the orientation of the crystalline blocks with respect to the principal directions of the film, the crystals sizes along the directions normal to the ($\bar{1}05$), (010) and (100) planes were studied. In the following, $L_{\bar{1}05}$ will be referred as the length, L_{010} the width and L_{100} the thickness of crystallites.

At the end of the first drawing, a molecular network is formed where small crystalline blocks act as permanent junction points [12,20,22,23,27,28]. Obviously, stretching

Table 1
Characteristics of samples drawn under constant force. λ_p corresponds to the apparent plateau draw ratio and λ_2 is defined as the effective draw ratio measured on the sample. The annealing time is the difference between the time needed to reach λ_p and the total duration of application of stress (5 s)

T (°C)	σ_0 (MPa)	λ_p	λ_2	Time to reach λ_p (s)	Annealing time (s)	$\dot{\epsilon}_{max}$ (s^{-1})	Time to reach $\dot{\epsilon}_{max}$ (s)
125	15	3.4	4.7	2.1	2.9	1.2	0.9
125	20	4.4	5.1	0.8	4.2	4.3	0.3
125	25	4.9	5.4	0.6	4.4	5.9	0.2
105	20	3.9	4.4	0.7	4.3	4.0	0.3
115	20	4.2	4.5	0.8	4.2	4.4	0.3
125	20	4.4	5.1	0.8	4.2	4.3	0.3

of the amorphous film leads to crystalline blocks in which the chain axis is mainly oriented along the draw (or X_1) direction. The transverse stretching of the monodrawn films tends to generate crystalline blocks whose chain axes are oriented along the new stretching direction X_2. Valuable informations on the deformation mechanisms can be obtained by studying the sizes of crystals having their chain axes aligned along X_1 or X_2 (X_1 or X_2 crystals, respectively) or which lie between the main directions (X_1 and X_2) of the film (''intermediate'' crystals). Despite their rather large distribution in the plane of the film, particular attention has been given at 45° with respect to the X_1 and X_2 directions.

3. Materials and transverse stretching

Rhône Poulenc Films provided one-way drawn PET films obtained on a pilot device by constant speed drawing at an initial strain rate of 0.5 s^{-1}, a stretching temperature of 91°C and a draw ratio equal to 4. The film was quenched on a cold roll after drawing.

3.1. Transverse stretching

Model samples of transversally stretched monodrawn films were obtained as follows. Samples with dimensions 100 × 20 mm^2 were cut from the one-way drawn films and stretched transversally to the first drawing direction (i.e. along the X_2 direction) under a constant drawing force on a specially designed equipment in the Saint Fons Research Centre of Rhône Poulenc. The samples were first preheated at the second stretching temperature during 10 s. Three different temperatures of stretching (105°, 115° and 125°C) and applied loads (15, 20, 25 MPa) were used. Several drawing characteristics are given in Table 1.

It can be noted that the engineering stretching stresses are by a factor 4 higher than those required to stretch amorphous samples under similar conditions of temperatures [20]. They are slightly higher than the yield stress measured by the transverse drawing at constant speed of one-way drawn films [29].

The samples were left under the applied load during 5 s which is enough for the sample to be stretched (see Table 1). Thermal quenching was then done by inflating room temperature air. The effective draw ratio was measured by means of a grid placed on the samples and only the central portion of the specimen, which was checked to be at constant width and homogeneously deformed, was considered for further characterization.

In order to understand the various types of samples that can be obtained, the kinetics of deformation has to be considered. Fig. 1 displays a typical evolution of the overall draw ratio versus time. The instantaneous strain rate $\dot{\epsilon}(t) = (1/\lambda)(d\lambda/dt)$ is also depicted. It can be seen, as it has been observed for the same type of stretching applied to amorphous films [20,30], that an equilibrium draw ratio (hereafter called the plateau draw ratio) is observed for given values of temperature and applied load. Under our experimental conditions, the plateau draw ratio is reached before 5 s. Therefore an annealing of a few seconds is applied under load at the stretching temperature. This annealing step avoids rupture of the samples when the thermal quenching is carried out. By varying the annealing time, it has been verified that the possible structural changes occurring during this step do not affect the molecular orientation which remains constant within the uncertainty of the measurements.

In order to follow the changes in molecular orientation before reaching the plateau deformation, several samples were obtained by stopping mechanically the extension

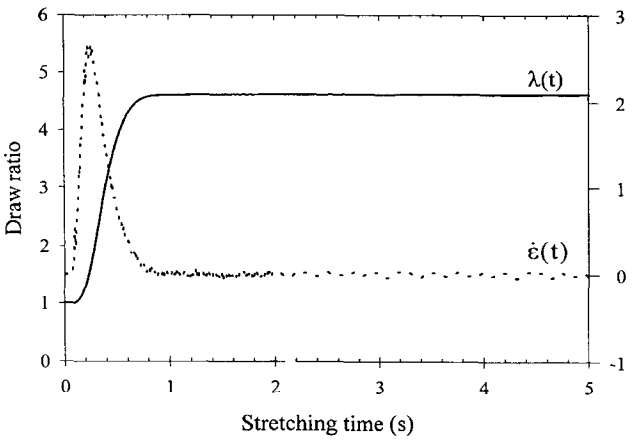

Fig. 1. Typical kinetics of deformation under a given applied load and temperature. Draw ratio (—) and strain rate (· · ·) versus stretching time.

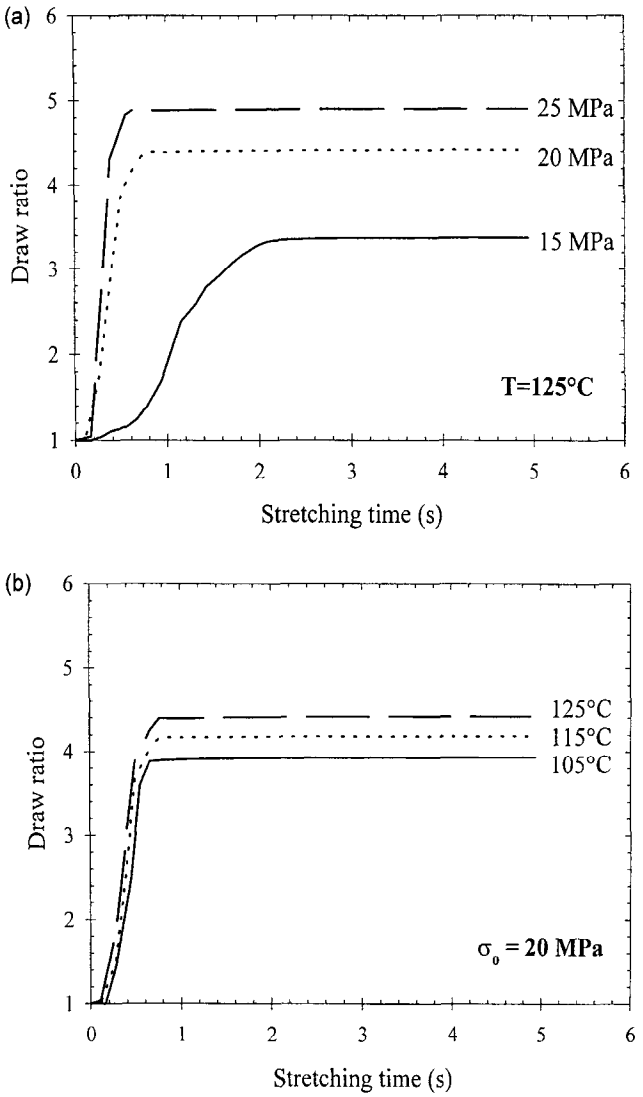

Fig. 2. (a) Draw ratio versus stretching time under different applied loads at 125°C. 15 MPa (—), 20 MPa (· · ·) and 25 MPa (- - -). (b) Draw ratio versus stretching time under an applied stress of 20 MPa at various draw temperatures. 105°C (—), 115°C (· · ·) and 125°C (- - -).

process. These samples will be referred as "quenched" samples. Due to the inhomogeneous deformation, it has been difficult to obtain reliable and reproducible samples drawn at low draw ratios ($\lambda < 2$).

4. Results

4.1. Kinetics of the stretching process

It can be seen in Fig. 1 that this stretching process is characterized by an unusual succession of strain rates. The stretching process starts with low strain rates. The strain rate then increases, goes through a maximum and decreases. At longer times, the stretching process stops and a plateau value of the deformation is obtained. This overall behavior is very similar to the constant force stretching of amorphous films although the two initial states are quite different [30]. Despite the existence of network type structure in the one-way drawn samples, the deformation occurs rapidly and high strain rates are reached (6 s^{-1} under an applied force of 25 MPa). Films with large second draw ratios can be obtained with this technique ($\lambda > 4$).

The influences of applied load and temperature on the kinetics of deformation are depicted in Fig. 2a and b, respectively. It appears that both an increase in applied load or stretching temperature lead to an higher value of the plateau draw ratio. As temperature increases, the kinetics of deformation are faster but this parameter has less influence than the applied stress (see Table 1). The true draw ratio as measured in the central part of the sample appears closer to the overall draw ratio (given on Fig. 2) as the temperature or the applied load increase which indicates that the stretching process becomes more homogeneous under these conditions.

4.2. Characterization of the starting materials

4.2.1. One-way drawn film

The crystalline structure of the one-way drawn film has been characterized following a previously described procedure and the main results are given in Table 2. As compared to model samples, obtained under similar conditions of strain rates and temperatures, characterized in previous studies [22], both the crystallinity and the chain axes orientation in the crystalline phase appear rather low.

4.2.2. Preheating

It has been shown that preheating might change significantly the crystallinity and other properties of the original sample [16]. The sample at the end of the preheating step corresponds to our reference in order to examine the orientation and morphology changes during further stretching. Therefore in foregoing figures, the data corresponding to the preheated sample will be set at $\lambda_2 = 1$. Whatever the temperature, the preheating allows an increase in crystallinity, which can be explained by the growth of the crystalline blocks mainly along their width and thickness directions as shown in Fig. 3. This increase is more important when temperature is higher, whereas the increase in crystal length is independent on the temperature of preheating. The competition between relaxation phenomena, which mainly act on the chain axis direction, and thermal crystallization both favored by a temperature increase can explain this behavior. On the contrary, the crystal growth towards the normals of (010) and (100) planes is only controlled by the thermal mobility.

4.3. Influence of the transverse stretching draw ratio

4.3.1. Crystallinity

At a given temperature, the molecular reorientation processes involved during stretching are carried out at constant

Table 2
Characterization of the one-way drawn film: crystallinity, sizes of crystals and orientation of the chain axes and of the normal to the phenyl ring

Morphology		Orientation	
χ (%)	17	$P_2^{\bar{1}05/X_1}$	0.37
L_{05} (nm)	3.6	$P_2^{\bar{1}05/X_3}$	−0.38
L_{010} (nm)	3.2	P_2^{100/X_1}	−0.34
L_{100} (nm)	2.2	P_2^{100/X_1}	0.69

crystallinity as shown in Fig. 4. The crystallinity raises with temperature without any influence of the draw ratio. This behavior is similar to what has been observed under constant speed drawing of one-way drawn samples.

4.3.2. Orientation

Fig. 5a and b show the evolution with the draw ratio of the second moments of the distribution function of the ($\bar{1}05$) and (100) plane normals, respectively. Fig. 5a clearly shows that the transverse drawing involves the orientation of the chain axes towards the new stretching direction (X_2) when the draw ratio λ_2 increases. By this way, less and less chain axes are aligned towards the X_1 direction. For large extensions, the orientation level of the chain axes along X_2 is almost the same as the orientation level along X_1 in the preheated sample. These reorientation mechanisms do not affect the high orientation level of the chain axes in the plane of the film. The data corresponding to the "quenched samples" indicate that the reorientation phenomena are efficient even at moderate extensions.

Fig. 5b shows a slightly more perpendicular orientation of the phenyl ring normals with respect to the X_2 direction which can be accounted for by the reorientation of the chain axes along X_2 since phenyl rings and chain axes are roughly perpendicular. At the same time, as the draw ratio increases, the (100) plane normals tend to be more and more parallel to the X_3 direction traducing an increased tendency

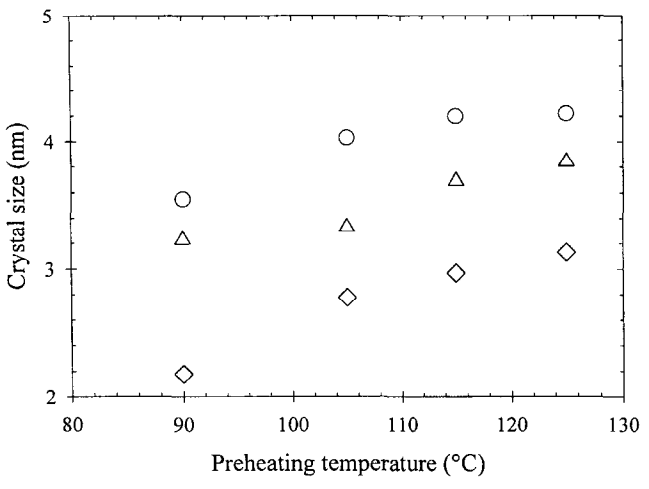

Fig. 3. Crystals length (○), width (△) and thickness (◇) versus preheating temperature for one-way drawn samples.

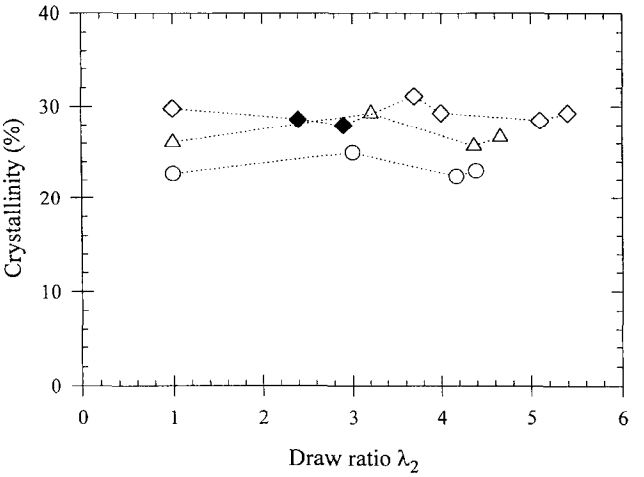

Fig. 4. Crystallinity (volume fraction) versus effective draw ratio at 105°C (○), 115°C (△), 125°). Black symbols represent the "quenched" samples and the open ones represent "equilibrium" samples.

of the phenyl rings to lie in the plane of the film as it has been observed for other types of stretching [15,16].

4.3.3. Orientation distribution

The reorientation of the chain axes towards the new stretching direction is not surprising for a sequential biaxial stretching. It has been largely described in the literature [15,17,31]. To analyze with more details the reorientation mechanisms, the diffracted X-ray intensity versus the in-plane-rotation angle ϕ_p is presented in Fig. 6 for various draw ratios. For $\lambda_2 = 1$, almost all the chain axes in the crystalline phase are oriented within a few degrees along the X_1 direction. Then, as the draw ratio increases, the measured intensity towards X_1 decreases rapidly. It can be seen that even for moderate draw ratios ($\lambda_2 = 2.4$), the initially along X_1 oriented crystals have almost disappeared. At the same time, the number of chain axes oriented with respect to the X_2 direction increases. At the highest draw ratios, it can be noted that the number of chain axes aligned along X_2 (in the crystalline phase) is much lower than the number of chain axes initially present along X_1. Since the stretching is carried out at an almost constant crystallinity, this implies that a significant fraction of the chain axes is lying at intermediate angles between X_1 and X_2.

Indeed a relative maximum appears for intermediate in-plane rotation angles ϕ_p. This maximum shifts towards the new stretching direction when λ_2 increases. These results might indicate that some initially along X_1 oriented crystals rotate towards X_2.

4.3.4. Length of the crystals in the plane of the film

In order to check this assumption, we investigated the crystal size along the ($\bar{1}05$) plane normals as a function of the directions in the plane of the film. The results are given on Fig. 7 for both samples drawn at the lowest draw ratios. The shape of the curves owes a great resemblance with that

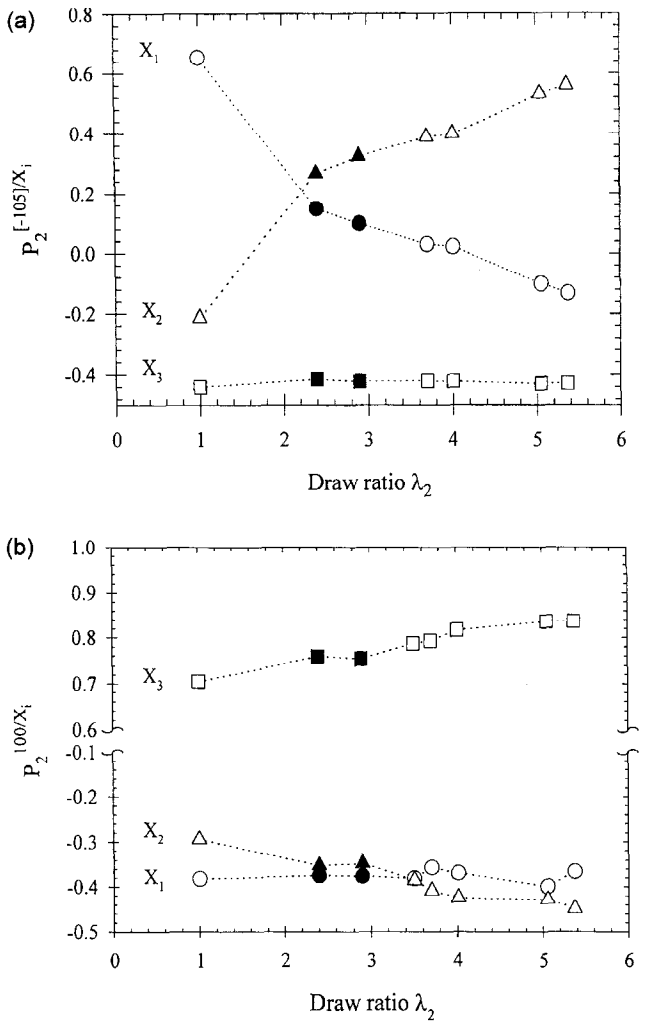

Fig. 5. (a) Orientation of $(\bar{1}05)$ planes normals versus draw ratio λ_2 with respect to X_1 (○), X_2 (△)) and X_3 (□) for samples stretched at 125°C. Black symbols represent the "quenched" samples and the open ones represent "equilibrium" samples. (b) Orientation of (100) planes normals versus draw ratio λ_2 with respect to the film directions for samples stretched at 125°C. Symbols are the same as in Fig. 4a.

of the X-ray intensity versus ϕ_p (Fig. 6). A large drop in the size of the crystals oriented along X_1 is observed at low draw ratios. The fact that a reliable measurement of size along this direction can be carried out is a good proof that some X_1 oriented crystals remain in the same direction after moderate draw ratios. The crystals that are oriented along the stretching direction X_2 show a relatively high length, which increases strongly with λ_2. It can be noted that at $\lambda_2 = 2.4$, the X_2 oriented crystals have almost the same length as the previously existing crystals lying along X_1. The length of the crystals also exhibits a relative maximum at intermediate angles. Its position is shifted towards X_2 as the draw ratio increases but its intensity does not seem affected. The relative maxima do not coincide exactly with those seen in the X-ray diffracted intensity distribution. They appear at lower angles for the size.

Fig. 8 shows the Bragg angle of the diffraction peak

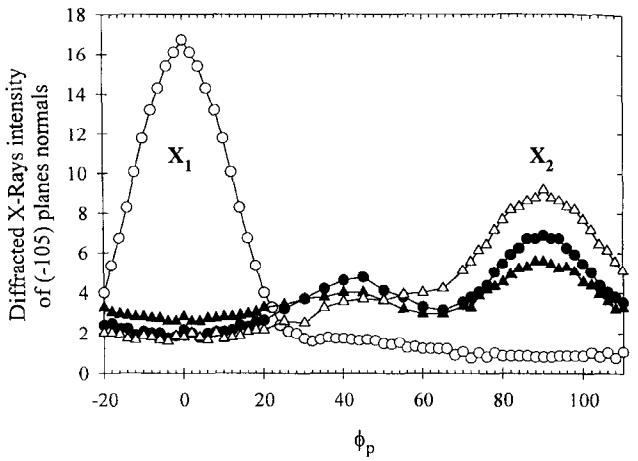

Fig. 6. Diffracted X-rays intensity of $(\bar{1}05)$ planes normals corrected from the background versus the in-plane-rotation angle at various draw ratios $\lambda_2 = 1$ (○), $\lambda_2 = 2.4$ (▲), $\lambda_2 = 2.9$ (●), $\lambda_2 = 3.7$ (△) for samples stretched at 125°C.

versus the in-plane rotation angle. The $2\theta_{\bar{1}05}$ increases and moves closer to the theoretical value calculated by Daubeny et al. [26] when ϕ_p increases. This behavior might indicate some degree of deformation of the unit cell under the stretching forces. The crystals oriented along the X_2 direction are larger and as perfect as those of the preheated sample. Previously existing crystals are partially broken and show lower crystalline perfection when deformation occurs.

Fig. 9 shows the crystal length of the three kinds of crystals versus the draw ratio λ_2 at 125°C. The X_1 crystals become shorter in the beginning of the deformation and disappear at high ratios. The length of the intermediate crystals was measured at $\phi_p = 45°$. It first increases at moderate extensions and decreases at higher extensions. The shift with the draw ratio of the position of the relative maximum seen in Fig. 7 may account for this behavior. On

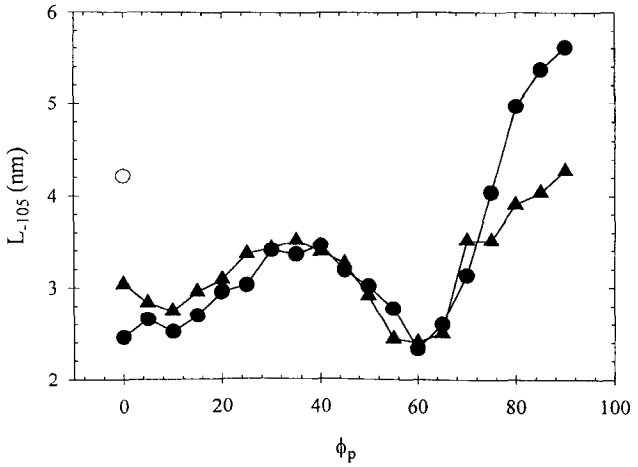

Fig. 7. Averaged crystal size along the $(\bar{1}05)$ planes normals versus the in-plane-rotation angle at various draw ratios $\lambda_2 = 1$ (○), $\lambda_2 = 2.4$ (▲), $\lambda_2 = 2.9$ (●) for samples stretched at 125°C.

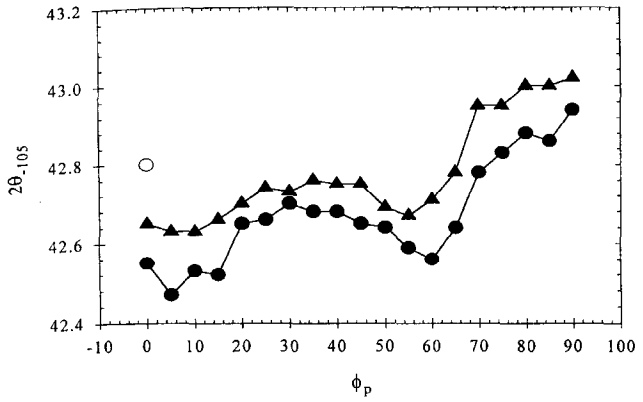

Fig. 8. The Bragg angle, $2\theta_{\bar{1}05}$, versus the in-plane-rotation angle at various draw ratios $\lambda_2 = 1$ (○), $\lambda_2 = 2.4$ (▲), $\lambda_2 = 2.9$ (●) for samples stretched at 125°C.

the contrary, the X_2 oriented crystals are long as soon as they appear and grow up as λ_2 increases.

4.3.5. Reorientation mechanisms

These results indicate rather complex reorientation mechanisms of the chain axes in the crystalline phase during stretching. The appearance of a relative maximum in the number of crystals (diffracted intensity) and in their length along ($\bar{1}05$) plane normals tends to show that crystals initially oriented along the X_1 direction in the monodrawn film are rotating towards the new stretching directions. Since the size of these intermediate crystals is somewhat lower than the initial length of the X_1 crystals, it can be thought that a partial erosion or melting of the X_1 crystals occurs, especially during the first stages of stretching. The appearance of long crystals oriented along X_2 even at moderate deformations can be explained by the growth along ($\bar{1}05$) plane normals of crystals that have been rotated during the stretching process.

The rotation mechanism would not be expected on the

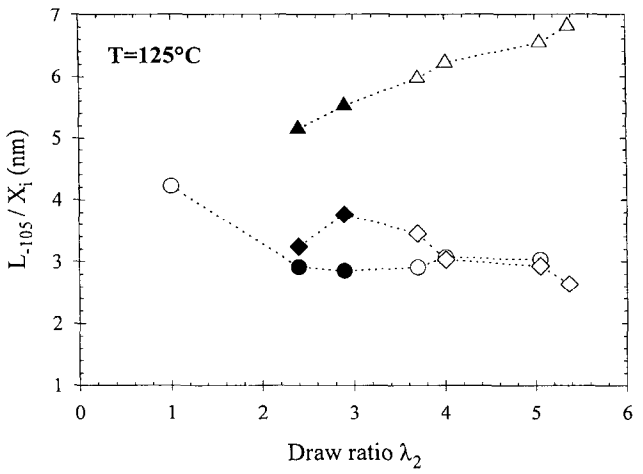

Fig. 9. Length of the X_1 (○), X_2 (△) and I (◇) crystals versus draw ratio λ_2 for samples stretched at 125°C.

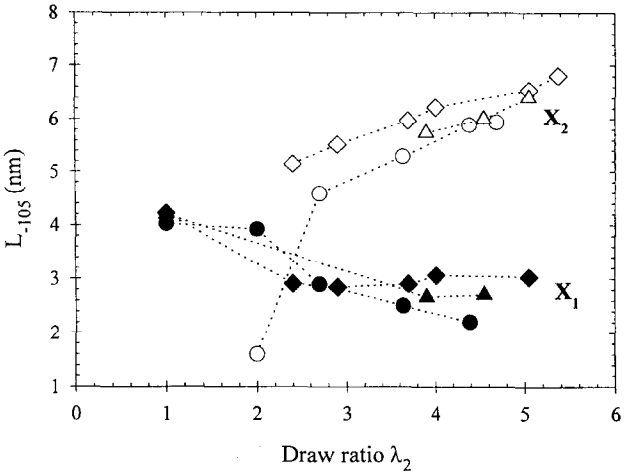

Fig. 10. Length of the X_1 (black symbols), X_2 (open symbols) crystals versus draw ratio λ_2 at 105°C (○), 115°C (△) and 125°C (◇).

basis of an affine or pseudo-affine deformation scheme. Its occurrence might originate from:

- first, the rotation of crystals that are not perfectly oriented along X_1 initially;
- secondly, a cooperative motion of the crystalline blocks which is helped by the rather rigid character of amorphous phase segments at the high deformation rates involved in the stretching process.

4.4. Influence of the stretching temperature

4.4.1. Length of the crystals

The influence of temperature on the length of the various types of crystals is depicted in Fig. 10. It can be seen that longer crystals are formed as temperature increases. However the breakage of the old crystals is more difficult at high temperature. The increase in crystal length can be understood by an increase in the crystallization kinetics at higher temperature. In the same way, destruction of crystals is more difficult as temperature increases for probably two reasons.

- higher tendency for crystallization at elevated temperatures;
- increase in temperature relaxes part of the stress carried by the amorphous chain segments.

4.4.2. Number of crystals

Fig. 11 shows the evolution of the crystal size along the (100) plane normals. The crystal thickness increases slightly with λ_2. In a first approximation, it is a unique function of the stretching temperature as it has been observed in other types of stretching [16,20]. Our data show a small increase of the thickness especially at low draw ratios.

The knowledge of crystal sizes ($L_{\bar{1}05}$, L_{010} and L_{100}) allows the calculation of the number of crystals per unit

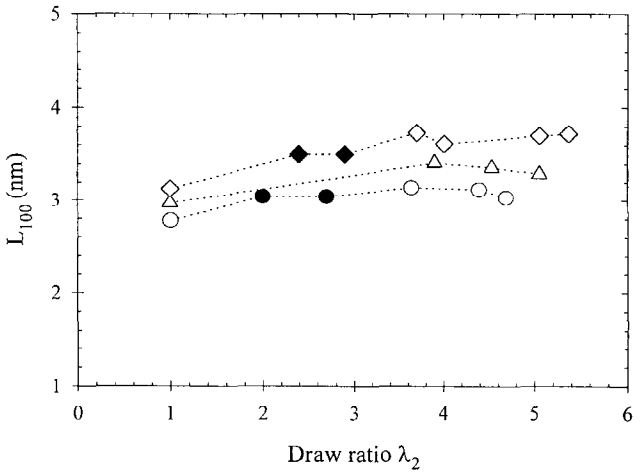

Fig. 11. Crystal size along the (100) planes normals versus draw ratio λ_2 at 105°C (○), 115°C (△) and 125°C (◇).

volume using the following expression:

$$N_{cr}(X_i) = w_i \frac{\chi_c}{L_{\bar{1}05} L_{100} L_{010}} \quad (4)$$

were w_i is the fraction of X_i oriented crystals. It is obtained by the relative intensity measured along each direction X_1 and X_2. This number was calculated for samples whose intermediate crystals are not significant, so for draw ratios higher than 3.5. As shown in Fig. 12, the number of old crystals decreases rapidly when the deformation proceeds. On the opposite, the number of new crystals does not depend on the stretching temperature nor on deformation.

4.4.3. Orientation

Fig. 13a and b shows the orientation of ($\bar{1}05$) plane normals with respect to the direction X_2 and X_1, respectively, at various temperatures. The orientation of the chain axes

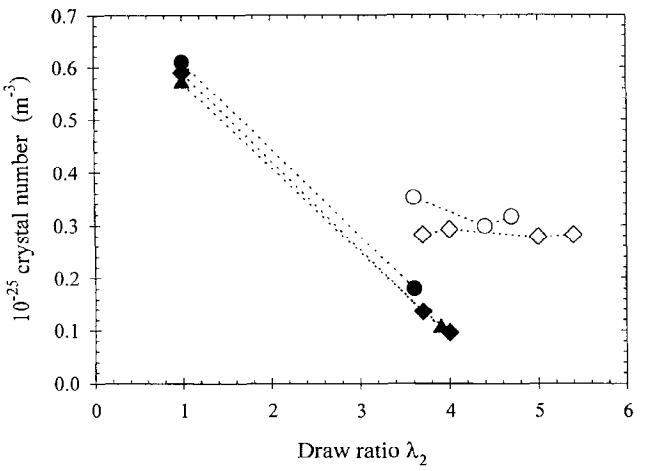

Fig. 12. Number of crystals per unit volume versus draw ratio λ_2 at 105°C (○), 115°C (△) and 125°C (◇) for X_1 (black symbols) and X_2 (open symbols) crystals.

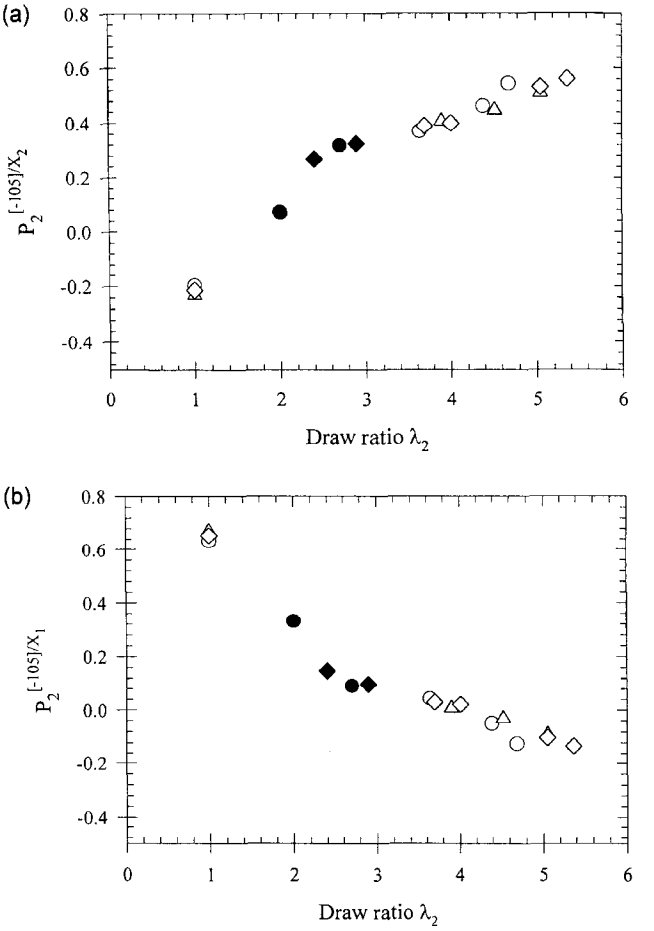

Fig. 13. Orientation level of (05) planes normals with respect to the second stretching direction and the first stretching direction respectively versus draw ratio at 105°C (○), 115°C (△) and 125°C (◇).

appears independent on the stretching temperature, within the accuracy of our measurements.

4.4.4. Conclusions

To conclude, constant force drawing involves rapid kinetics. For example, the strain rate could reach a maximum of 6 s^{-1} at 125°C for an applied load of 25 MPa (Table 1). High strain rates inhibit relaxation mechanisms and allow an efficient rearrangement of the initial network obtained at the end of the first drawing step. Initial crystals oriented along X_1 are broken and/or rotated towards the new stretching direction when they are still large. Therefore, new crystals oriented along X_2 are long and with a high crystalline perfection as soon as they appear. However, since $L_{\bar{1}05}$ is averaged over all the crystalline phase, the formation of new small crystals by nucleation and growth mechanism could not be excluded. It is however not a dominant mechanism. No relaxation phenomena can be detected in the crystalline phase probably because of the high strain rates involved and the predominance of rotation phenomena which do not destroy the junctions of the molecular network.

5. Comparison with constant speed drawing

In this section, we would like to emphasize the main difference between constant force stretching and extension under controlled strain rate. This corresponds practically to a comparison between the second drawing stages of the "inverse" and "balanced" industrial processes. Although the one-way drawn films used in both studies are slightly different, making difficult a quantitative comparison of the two stretching processes, some important and clear qualitative differences can be established.

A first difference, at least observed on model samples, concerns the achievable draw ratios. Under constant speed drawing, it has been experimentally noted that only limited extensions can be achieved before the film breakage (up to $\lambda_2 = 4$ under an initial nominal strain rate equal to 0.25 s^{-1} [15,16]). Constant force stretching may lead to higher draw ratios by increasing temperature or applied load.

The state of orientation of the chain axes and its evolution with the draw ratio appear also slightly different. First, no relative maximum at intermediate directions of the film plane is observed for constant speed drawing. The X-ray diffracted intensity of X_1 crystals ($(\bar{1}05)$ plane normals aligned along X_1) decreases smoothly with draw ratio leading to bimodal distributions of diffracted intensity even if the draw ratio is as large as 4. The number of chain axes (in the crystalline phase) oriented along the X_1 or X_2 direction is on the same order of magnitude. For a given draw ratio, more chain axes are still aligned towards the first stretching direction in constant speed drawing as compared with constant stress extension.

This latter process appears more efficient in reorienting crystalline chain axes towards the stretching direction. The high strain rates, encountered with this type of stretching, might explain this behavior.

Differences between the two processes also exist as far as the crystal length is concerned. For imposed strain rate drawing, the length of crystals oriented along X_1 decreases and the length of new crystals aligned along X_2 increases slowly. Crystals, lying either along X_2 or at intermediate directions, are smaller than those initially present (aligned along X_1) as soon as they can be experimentally detected. On the contrary, under constant stress stretching, we have shown that rather long crystals oriented along X_2 can be evidenced even at moderate draw ratios.

The results indicate different mechanisms for the formation of the new crystalline network. Under constant speed drawing, the new crystals are formed by the occurrence of two processes:

- a nucleation and growth process due to stress induced crystallization of ordered chain axes of the amorphous phase preferentially aligned towards X_2;
- a growth process based on small crystals remaining from a partial breakdown of crystalline blocks having their chain axes oriented along X_1.

Under constant force drawing, probably because of the rapid deformation kinetics, no relaxation takes place, and breakage of initially present crystalline blocks does not seem to be predominant. On the other hand, rotation of large crystals towards X_2 occurs. These crystals can further grow up as the draw ratio increases. Since the stretching is carried out under constant crystallinity, some initial crystals (aligned along X_1) have to disappear.

In both types of stretching, an increase in drawing temperature leads to an higher crystallinity and bigger crystals along all the investigated crystallographic directions. However, under constant speed, a slight relaxation of orientation with temperature can be observed, whereas the orientation in the crystalline phase is uniquely controlled by the draw ratio in the other stretching process.

6. Conclusions

The development of the orientation of the chain axis and the normal to the phenyl ring in the crystalline phase has been characterized for a second drawing process of sequentially drawn PET films, which has the peculiarity to be conducted under constant force.

It has first been shown that large extensions can be obtained using stresses above the yield stress (measured along the second draw direction) of the monodrawn film. A molecular network is formed with crystalline blocks acting as junctions, which leads to an equilibrium deformation under given conditions of temperature and applied stress.

The main features of this stretching process are:

- an extremely rapid decrease of the number of crystalline chain axes oriented perpendicularly to the stretching direction;
- the appearance, at moderate extensions, of a significant population of crystals with their chain axes oriented at intermediate angles between the first and the second drawing directions;
- an important length of crystals oriented at intermediate angles and an even larger one for crystals oriented along the new stretching direction;
- an orientation level of chain axes and phenyl ring normal that is uniquely controlled by the draw ratio, without any relaxation effects with temperature.

References

[1] Bonnebat C, Roullet G, De Vries AJ. Polym Engng Sci 1981;21:189.
[2] Cakmak M, Spruiell JE, White JL. Polym Engng Sci 1984;24:1390.
[3] Schmidt FM, Agassant JF, Desoutter L. J Non Newtonian Fluid Mech 1996;64:19.
[4] De Vries AJ, Bonnebat C, Beautemps J. J Polym Sci, Polym Symp 1977;58:109.
[5] Cakmak M, Spruiell JE, White L, Lin JS. Polym Engng Sci 1987;27:893.

[6] Cakmak M, White JL, Spruiell JE. Polym Engng Sci 1989;29:1534.
[7] Gohil RM, Salem DR. J Appl Polym Sci 1989;1993:47.
[8] Gohil RM. J Appl Polym Sci 1993;48:1635.
[9] Gohil RM. J Appl Polym Sci 1993;48:1649.
[10] Yoshihara N, Fukushima A, Watanabe Y, Nakai A, Nomura S, Kawai H. J Soc Fiber Sci Tech (Japan) 1981;17:T–387.
[11] Chandran P, Jabarin S. Adv Polym Technol 1993;12:119.
[12] Chandran P, Jabarin S. Adv Polym Technol 1993;12:133.
[13] Chandran P, Jabarin S. Adv Polym Technol 1993;12:153.
[14] Lee KH, Sung CSP. Macromolecules 1993;26:328.
[15] Faisant de Champchesnel JB, Bower DI, Ward IM, Tassin JF, Lorentz G. Polymer 1993;34:3763.
[16] Faisant de Champchesnel JB, Tassin JF, Bower DI, Ward IM, Lorentz G. Polymer 1994;35:4092.
[17] Faisant de Champchesnel JB, Tassin JF, Monnerie L, Sergot P, Lorentz G. Polymer 1997;38:4165.
[18] Dargent E, Grenet J, Auvray X. J Thermal Anal 1994;41:1409.
[19] Marquez-Lucero A, G'Sell C. Polymer 1993;34:2740.
[20] Lapersonne P, Tassin JF, Monnerie L, Beautemps J. Polymer 1991;32:3331.
[21] Lapersonne P, Tassin JF, Monnerie L. Polymer 1994;35:2192.
[22] Vigny M, Tassin JF, Gibaud A, Lorentz G. Polym Engng Sci 1997;37:1785.
[23] Ajji A, Cole KC, Dumoulin MM, Brisson JC. Polymer 1995;36:4023.
[24] Ajji A, Guevremont J, Cole KC, Dumoulin MM. Polymer 1996;37:3707.
[25] Fu Y, Busing WR, Jin Y, Affholter KA, Wunderlich B. Macromol Chem Phys 1994;195:803.
[26] de Daubeny R, Bunn CW, Brown JC. J Proc R Soc A 1954;226:531.
[27] Salem DR. Polymer 1992;33:3182.
[28] Padibjo SR, Ward IM. Polymer 1983;24:1103.
[29] Faisant de Champchesnel JB. Ph.D. Thesis, University Pierre et Marie Curie, Paris VI, 1994.
[30] Lebourvellec G, Beautemps J, Jarry JP. J Appl Polym Polym Sci 1990;39:319.
[31] Chang H, Schultz JM, Gohil RM. J Macromol Sci Phys 1993;B32:99.